IJDIAS International Journal of Discoveries and Innovations in Applied Sciences

| e-ISSN: 2792-3983 | www.openaccessjournals.eu | Volume: 3 Issue: 8

A Noise Density-Based Fuzzy Approach for Detecting and Removing Random Impulse Noise in Color Images

Adel Jalal Yousif

University of Diyala, Diyala, Iraq

Abstract:

This paper introduces a new approach aimed at restoring images corrupted by random valued impulse noise. The adopted methodology leverages fuzzy logic and encompasses three primary stages: estimation of noise density, detection of fuzzy noise, and reduction of fuzzy noise. Within the fuzzy noise detection phase, a fuzzy set labeled as "Noise-Free" is formulated through the utilization of the rank-ordered mean of absolute differences and the estimated noise density. This set serves to discern whether a given pixel should be classified as noisy or noise-free. Utilizing the fuzzy logic in the proposed method collaborates to determine the ultimate fuzzy weight assigned to each pixel, thereby facilitating the restoration of corrupted image pixels. Empirical results based on peak signal-to-noise ratio, mean square error, and visual assessment demonstrate the effectiveness of the proposed technique in suppressing noise, preserving fine details, and surpassing the performance of several established filtering methods.

1. Introduction

In numerous digital image processing applications, the captured images often suffer from noise corruption, stemming from issues during image transmission or acquisition. Noise degradation diminishes image quality and introduces adverse effects into subsequent image processing stages, including segmentation, parameter estimation, and enhancement. Consequently, the elimination of noise from images emerges as a fundamental and critical task within the domain of image processing. Impulse noise, characterized by brief 'on/off' noise pulses of relatively short duration, holds a significant and pervasive presence among digital image noise sources. Its impact is felt during image acquisition due to factors like noisy sensors (arising from switching or sensor temperature variations), as well as during transmission due to channel imperfections (interference, atmospheric disturbances), hardware-related defects, or synchronization errors during analog-to-digital conversion within image processing workflows. This study specifically focuses on the Random Valued Impulse Noise (RVIN) model of impulse noise [1-5].

Among the diverse techniques for mitigating impulse noise, the median filter [6,7] has gained popularity due to its effective noise suppression capabilities coupled with high computational efficiency. However, the median filter often suffers from drawbacks such as destroying image details and introducing blurring, as each pixel is replaced with the median value of its surrounding neighborhood. To address this issue, several forms of adaptive and center-weighted median filter [8-15] was introduced, which assigns greater emphasis to the central pixel within the observed window. Although this modification preserves more image details than the median filter, it uniformly treats all pixels across the image, without distinguishing between noisy and noise-free pixels. This paper introduces a new approach for removing RVIN from images. The proposed method employs fuzzy techniques alongside estimated noise density. The estimation of noise density serves dual purposes: first, to determine the appropriate window size for the fuzzy noise detection step, and second, to shape the membership function used in the fuzzy noise detection process. The fuzzy logic, which is adopted by Zadeh in 1965, is a mathematical tool for dealing

IJDIAS International Journal of Discoveries and Innovations in Applied Sciences
| e-ISSN: 2792-3983 | www.openaccessjournals.eu | Volume: 3 Issue: 8

with uncertainty. It presents a crucial model of computing with words and furnishes an approach for handling imprecision and information granularity within the realm of soft computing [16-20].

2. RVIN Model

Impulse noise inherently maintains its independence and lacks correlation with individual image pixels, resulting in a subset of pixels bearing noise while the remainder remains untarnished. When dealing with random valued impulse noise, colloquially termed uniform impulse noise, the affected pixels can adopt any value within the gray level spectrum, denoted as $[Lmin, Lmax]$ in an 8-bit image representation. Consequently, these noisy pixels span the full gray level range from 0 to 255. This scenario entails a stochastic dispersal of noise throughout the entire image, leading to an equal probability of any given gray level value manifesting as noise. The Random Valued Impulse Noise (RVIN) model can be briefly described as follows [21, 22]:

$$I(x,y) = \begin{cases} n(x,y), & \text{with probability } P \\ O(x,y), & \text{with probability } 1-P \end{cases} \quad \text{... (1)}$$

Where, (x,y) is the noisy image pixel, $n(x,y)$ is the noisy impulsive pixel at position (x,y), and (x,y) is the uncorrupted (original) image pixel.

3. Proposed Method

The proposed method consists of four main concepts: estimation of noise density, noise detection, noise removing, and iterative processing which are described below in details.

3.1. Estimation of Noise Density

For estimating RVIN density in color image, each channel (color component) is processed separately by dividing it into 16 non-overlapping blocks (Bi) with i ∈ {1,2,…,16} and then the noise density for each block in each channel is calculated as described below for the first block (B_1) only but it is performed in an analogous way for the others:

1- Calculating the standard deviation (std_1) for the entire block B_1 based on the following equation:

$$std_1 = \sqrt{\frac{1}{(\grave{M}\times\grave{N})}\sum_{(x,y)\in B_1}\left(\grave{I}(x,y)-m_1\right)^2} \quad \text{... (2)}$$

B_1

where, m_1 : is the mean value of first block B_1

$\grave{I}(x,y)$: is the pixel data inside B_1 .

2- Scanning the whole image block B_1 using a 3x3 sliding window from pixel to pixel and using the following three steps in each scan:

i) $D_{xy}^{N4} = \left|\grave{I}(x+s,y+t) - \grave{I}(x,y)\right|$ with $s,t \in S_{N4}$ …(3)

Where, D_{xy}^{N4} represents the set of absolute differences between the central pixel and its four nearest neighbors within the processed window and

S_{N4} denotes the set of coordinates for the four neighbors of $I(x,y)$ given by:

$$S_{N4} = \{(-1,0),(1,0),(0,-1),(0,1)\} \quad \text{... (4)}$$

IJDIAS International Journal of Discoveries and Innovations in Applied Sciences

| e-ISSN: 2792-3983 | www.openaccessjournals.eu | Volume: 3 Issue: 8

Then the elements in D_{xy}^{N4} can be arranged in ascending order by value:

$$d_{xy}^{1} \leq d_{xy}^{2} \leq d_{xy}^{3} \leq d_{xy}^{4}$$

ii) Defining v_{xy} which represents the mean value of the second and third ordered elements in D_{xy}^{N4} by the following equation:

$$v_{xy} = \frac{d_{xy}^{2} + d_{xy}^{3}}{2} \qquad \text{... (5)}$$

iii) Using the standard deviation (std) of the processed image block and the value of v_{xy} to identify the current pixel $I(x, y)$ as follows:

$$M_{\mathrm{RV}}(x, y) = \begin{cases} 1, v_{xy} > std_1 \\ 0, v_{xy} \leq std_1 \end{cases} \qquad \text{... (6)}$$

Where, $M_{\mathrm{RV}}(x, y)$ denotes the decision rule for estimating RVIN density.

3- The noise density ND_{RV} for the first block is given as:

$$ND_{\mathrm{RV}}^{\mathrm{B1}} = CF \times \frac{\sum_{(x,y)\in \mathrm{B}_1} M_{\mathrm{RV}}(x, y)}{(\grave{M} \times \grave{N})_{\mathrm{B}_1}} \times 100\% \qquad \text{... (7)}$$

Where $\grave{M}_{\mathrm{B1}} \times \grave{N}_{\mathrm{B1}}$ denotes the size of the block B_1 , and CF denotes the control factor which is estimated by experiments $CF = 1.35$ (see table 1).

4- The calculation of the noise density for the other image blocks is done in the same way as for ($ND_{\mathrm{RV}}^{\mathrm{B1}}$) . Then, define the minimum value of ($ND_{\mathrm{RV}}^{\mathrm{B}i}$) as:

$$ND_{min} = \min_{1\leq i\leq 16} \left(ND_{\mathrm{RV}}^{\mathrm{B}i}\right) \quad , \text{ with } i \in \{1,2, \dots, 16\} \qquad \text{...(8)}$$

5- If ND_{min} is less than one, then the image is classified as clean. Otherwise, the image is classified as corrupted with RVIN. In this case, the overall noise density of the image equals to the mean value of the noise densities across all blocks and expressed is as follows:

$$ND_{\mathrm{RV}} = \begin{cases} 0 \text{ , if } ND_{min} < 1 \\ \mathrm{mean}_{1\leq i\leq 16}\left(ND_{\mathrm{RV}}^{\mathrm{B}i}\right) \text{ otherwise} \end{cases} \qquad \text{... (9)}$$

Where, ND_{RV} is the RVIN density for the entire channel.

3.2. Nosie Detection

As stated in section 2, in the context of RVIN, a noisy pixel holds the potential to exhibit any value within the gray level range [0-255] for an 8-bit image representation. Additionally, it might slightly deviate in intensity from the original value. Consequently, mitigating such noise presents a greater challenge compared to dealing with salt and pepper noise, necessitating a robust detection strategy. The proposed method employs the Rank-Ordered Mean of the Absolute Differences (ROMAD) in conjunction with estimated noise density, integrating the principles of fuzzy logic. The process of calculating the rank-ordered mean difference involves the central pixel's comparison with its neighboring pixels within a sliding window of dimensions $(2K+1)\times(2K+1)$, encompassing each pixel in the image. The value of K is dynamically determined based on the prevailing noise density:

IJDIAS International Journal of Discoveries and Innovations in Applied Sciences
| e-ISSN: 2792-3983 | www.openaccessjournals.eu | Volume: 3 Issue: 8

K is set to 1 when (NN RV<35%) and otherwise, it takes on the value of 2. To compute (ROMAD) for a given pixel (x,y), the following three steps are executed:

1- Compute the absolute differences, denoted as D_{xy} between the current pixel $I(x,y)$ and neighboring pixels within the observed window using the following formula :

$$D_{xy} = |I(x+s,y+t) - I(x,y)| \text{ with } s,t \in \{-K, \dots, +K\}, (s,t) \neq (0,0) \dots \qquad \dots(10)$$

Where, $I(x+s,y+t)$ denotes the pixels values within the processed window.

2- Assume d_{xy}^{i} be the ith smallest ranked value in D_{xy} when the elements of D_{xy} are arranged in ascending order, such that

$$d_{xy}^{1} \leq d_{xy}^{2} \leq \cdots \leq d_{xy}^{u}$$

Where, u is the number of the central pixel neighbors in the processed window $(2K+1) \times (2K+1)$. So, $u = ((2K+1)^2 - 1\ )$

3- The (ROMAD) for the current pixel is defined as:

$$R_{xy} = \frac{\sum_{i=1}^{n} d_{xy}^{i}}{n} \qquad \dots(11)$$

Where, $n = u - 2(2K-1)$ ... (12)

Upon completing the calculation of ROMAD for every pixel within the image, the ROMAD value serves as a valuable metric for discerning between pixels that are affected by noise and those that remain noise-free. Specifically, in scenarios where the noise ratio is low and the ROMAD value for a given pixel I(x,y) is small, it signifies that the pixel is noise-free and exists within a homogenous neighborhood. Conversely, a larger ROMAD value suggests that the pixel may be noisy or situated on an edge. Consequently, a fuzzy set labeled "Small ROMAD" is introduced to capture the linguistic notion of "small," and its membership function, denoted as μ_{small} and illustrated in figure 1, is employed to identify noise-free pixels. However, a challenge arises when dealing with high noise ratios, leading to consistently elevated ROMAD values. To address this issue, the membership function μ_{small} for the "Small ROMAD" fuzzy set can be dynamically shaped (i.e., its parameters determined) for each neighborhood. This adaptability is governed by two key criteria: firstly, the homogeneity level (H_{xy})of the neighborhood surrounding the tested pixel I(x,y). Secondly, the overall noise density of the entire image.

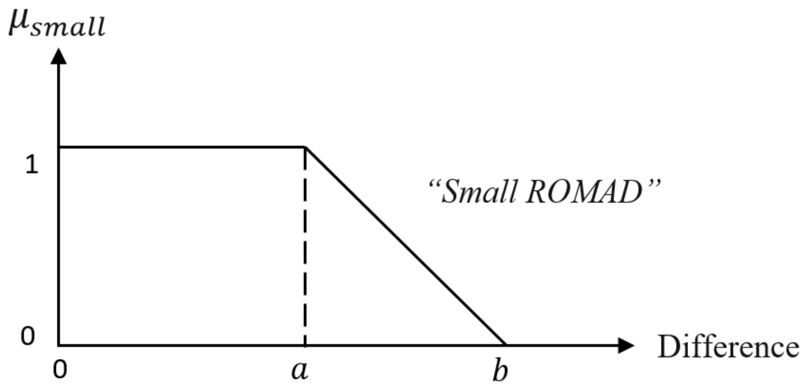

Fig.1: Membership function of fuzzy set *"Small ROMAD"*

The following equation describing the membership function μ_{small} :

$$\mu_{small}(R_{xy}) = \begin{cases} 1, R_{xy} < a \\ \frac{b-R_{xy}}{b-a}, a \leq R_{xy} \leq b \\ 0, R_{xy} > b \end{cases} \quad \dots (13)$$

Where:

$$a = H_{xy} \times NF_{\mathrm{RV}} \quad \dots (14)$$

$$b = q \times NF_{\mathrm{RV}} \quad \dots (15)$$

NF_{RV} denotes the noise factor and q represents the nth smallest value in $R_{(x+s,y+t)}$.

Further, the following steps describing how H_{xy} , NF_{RV} and q can be obtained:

Firstly, H_{xy} can be computed by utilizing the ROMAD values in the observed window as:

1- Assume r_i be the ith smallest ranked value in $R_{(x+s,y+t)}$ when the elements of $R_{(x+s,y+t)}$ are arranged in ascending order, such that:

$$r_1 \leq r_2 \leq \cdots \leq r_u$$

Where, $u = ((2K + 1)^2 - 1\ )$

2- obtain the value of H_{xy} as:

$$H_{xy} = \frac{\sum_{i=1}^{n} r_i}{n} \quad \dots (16)$$

Secondly, the value of q is obtained as:

$$q = r_n \quad \dots (17)$$

Thirdly, the value of NF_{RV} can be calculated by utilizing the straight line equation as illustrated in figure 2 and using the following expression:

$$NF_{\mathrm{RV}} = \frac{P_1 * (P_3 - ND_{\mathrm{RV}})}{P_3 - P_2} \quad \dots (18)$$

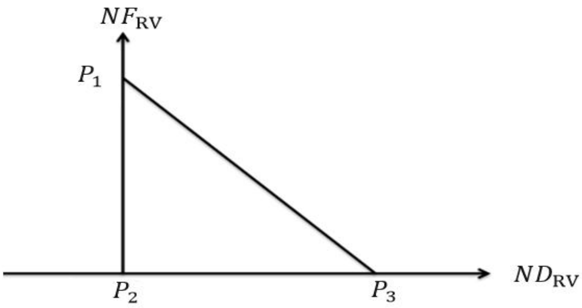

Fig. 2: The function of NF_{RV}

Where the parameters ($P1$, $P2$, and $P3$) are determined through experimental investigations. Empirical findings have indicated that the optimal values for these parameters are set to (2.9, 0, 61) respectively when the estimated noise density remains at or below 35%. Conversely, when the estimated noise density surpasses 35%, the parameters ($P1$, $P2$, and $P3$) are optimized at values of (1.9, 20, 100) respectively.

| e-ISSN: 2792-3983 | www.openaccessjournals.eu | Volume: 3 Issue: 8

Lastly, for each tested pixel $I(x,y)$, a fuzzy set *"Noise-Free"* is generated using the following fuzzy rule:

Fuzzy Rule 1: Defined when a central pixel $I(x,y)$ is a noise free pixel:

IF R_{xy} is *small*

THEN the central pixel $I(x,y)$ is *noise- free*

This rule can be applied by employing the equality operation between two fuzzy sets. As a result, the membership function of the fuzzy set *"Noise-Free"* is calculated as:

$$\mu_{noisefree}(I(x,y)) = \mu_{small}(R_{xy}) \quad \text{... (19)}$$

3.3 Noise Removing

The noise removing step is demonstrated for the red component only (i.e., C_{R}) but it is implemented in an analogous way for the other components. Hence, assume that $C_{\mathrm{R}}(x,y)$ is a noisy pixel (i.e. $\mu_{noisefree}(C_{\mathrm{R}}(x,y) < 1)$) and $F_{\mathrm{R}}(x,y)$ is the corresponding pixel of the filtered red component, and then one of the following cases will be applied for restoring the noisy pixel as follows:

Case1: IF $\left(\mu_{noisefree}(C_{\mathrm{G}}(x,y) < 1) \text{ AND } \mu_{noisefree}(C_{\mathrm{B}}(x,y) = 1)\right)$

$$F_{\mathrm{R}}(x,y) = \max(\min(C_{\mathrm{B}}(x,y) + \Delta_{RB}(x,y), 255), 0) \quad \text{... (20)}$$

Case2: IF $\left(\mu_{noisefree}(C_{\mathrm{G}}(x,y) = 1) \text{ AND } \mu_{noisefree}(C_{\mathrm{B}}(x,y) < 1)\right)$

$$F_{\mathrm{R}}(x,y) = \max(\min(C_{\mathrm{G}}(x,y) + \Delta_{RG}(x,y), 255), 0) \quad \text{... (21)}$$

Case3: IF $\left(\mu_{noisefree}(C_{\mathrm{G}}(x,y) = 1) \text{ AND } \mu_{noisefree}(C_{\mathrm{B}}(x,y) = 1)\right)$

$$F_{\mathrm{R}}(x,y) = \max\left(\min\left(0.5\left(C_{\mathrm{G}}(x,y) + \Delta_{RG}(x,y) + C_{\mathrm{B}}(x,y) + \Delta_{RB}(x,y)\right), 255\right), 0\right) \quad \text{... (22)}$$

Case4: IF $\left(\mu_{noisefree}(C_{\mathrm{G}}(x,y) < 1) \text{ AND } \mu_{noisefree}(C_{\mathrm{B}}(x,y) < 1)\right)$

$$F_{\mathrm{R}}(x,y) = \left(1 - \mu_{noise\ free}C_{\mathrm{R}}(x,y)\right) \times \frac{\sum_{s=-K}^{K}\sum_{t=-K}^{K} C_{\mathrm{R}}(x+s,y+t).\mu_{noise\ free}C_{\mathrm{R}}(x+s,y+t)}{\sum_{s=-K}^{K}\sum_{t=-K}^{K} \mu_{noise\ free}C_{\mathrm{R}}(x+s,y+t)} + \left(\mu_{noise\ free}C_{\mathrm{R}}(x,y)C_{\mathrm{R}}(x,y)\right) \quad \text{... (23)}$$

Where, $C_{\mathrm{R}}(x+s,y+t)$ represents the pixels values in the considered window of size $(2K+1)\times(2K+1)$. The size of observed window is selected adaptively according to the number of the noise free pixel in that window starting with $W=1$. If the observed window is fully noisy, then the size of window will be increased until the condition $(G_{xy}^{f_2} > 0)$ is met.

$$G_{xy}^{f_2} = \sum_{s=-K}^{K}\sum_{t=-K}^{K} C_{\mathrm{R}}(x+s,y+t) \text{ with } \mu_{noisefree}\left(C_{\mathrm{R}}(x+s,y+t)\right) = 1 \quad \text{... (24)}$$

3.4 Iterative Processing

During the noise detection stage, the membership functions μ_{small}, as illustrated in figure 1, dynamically adjust their shape based on the estimated noise density. Consequently, the proposed algorithms are executed in an iterative manner with two iterations. This iterative approach aims to enhance noise removal while preserving the details of image. In the second iteration, the altered image obtained from the initial iteration is utilized

IJDIAS International Journal of Discoveries and Innovations in Applied Sciences

| e-ISSN: 2792-3983 | www.openaccessjournals.eu | Volume: 3 Issue: 8

4. Experimental Results

Identifying a suitable parameter is a very significant task to obtain successful filtering results. Hence, different experiments have been implemented to select the best values for the control factor CF Eq. (7) which has a significant effect on the result of the noise density estimation. Table 1 contain different noise levels with parameters varying over a range of possible values for the "Peppers" image. It is clear from table 1 that the best value of the parameter CF equal to 1.35, where the difference between the estimated noise density and the real noise density is less than 5%. Hence, the suggested value is CF =1.35.

Table 1: Determination of parameter CF on "Peppers" image

Color components	Parameter values	Real Noise Density (RVIN)					
		10%	20%	30%	40%	50%	60%
Red component	0.95	7.8%	15.0%	22.0%	29.2%	35.4%	40.1%
	1.15	9.4%	18.1%	26.7%	35.3%	42.9%	48.6%
	1.35	11.0%	21.3%	31.3%	41.5%	50.4%	57.0%
	1.55	12.7%	24.5%	35.9%	47.6%	57.8%	65.5%
	1.75	14.3%	27.6%	40.6%	53.8%	65.3%	73.9%
Green component	0.95	5.9%	12.5%	19.4%	25.9%	33.0%	38.8%
	1.15	7.1%	15.2%	23.6%	31.4%	39.9%	46.9%
	1.35	8.4%	17.8%	27.7%	36.9%	46.9%	55.1%
	1.55	9.7%	20.5%	31.8%	42.3%	53.9%	63.3%
	1.75	10.9%	23.1%	35.9%	47.8%	60.8%	71.5%
Blue component	0.95	7.2%	15.1%	22.4%	29.3%	35.8%	40.7%
	1.15	8.8%	18.3%	27.2%	35.5%	43.4%	49.3%
	1.35	10.3%	21.5%	31.9%	41.7%	50.9%	57.9%
	1.55	11.9%	24.7%	36.7%	47.8%	58.5%	66.5%
	1.75	13.4%	27.8%	41.4%	54.0%	66.0%	75.0%

The performance evaluation of the suggested method involves a comparison with several existing noise reduction methods: DWM [23], HFC [24], CAFSM [25], and FMVMF [26]. Furthermore, the same proposed method is applied to grayscale images without incorporating the color differences step, termed as proposed (gray) in this section. Table 2 presents the quantitative outcomes of objective quality measurements, specifically Mean Squared Error (MSE) and Peak Signal-to-Noise Ratio (PSNR) [27-30], for the "Peppers" image (refer to figure 4). This image is subjected to corruption by 10%, 30%, and 50% RVIN. It is obvious from table 1 that the proposed color image algorithm has a superior performance as compared with the other noise reduction methods and with the proposed gray scale image algorithm as well. The impact of noise density on the proposed algorithm's performance, as well as the performances of related methodologies in terms of PSNR, is visualized in figure 3. While, figure 4 illustrates the noise filtering and detail preservation of the proposed method as compared with other methods. It is obvious from figure 4 that the proposed color image algorithm obtains the best result in low and high noise densities due to the following main reasons:

1. Adaptive Window Size: The utilization of an adaptive window size during both the noise detection and noise filtering stages is informed by the number of noise-free pixels present within the observed window.

IJDIAS International Journal of Discoveries and Innovations in Applied Sciences
| e-ISSN: 2792-3983 | www.openaccessjournals.eu | Volume: 3 Issue: 8

2. Color Component Correlation: Exploiting the inter-correlation between color components during the noise filtering stage. So, for restoring a certain noisy pixel $C_R(x,y)$ at position(x,y), the corresponding pixels in the other components i.e., ($C_G(x,y)$ and $C_B(x,y)$) are used instead of the neighbors pixels for $C_R(x,y)$.
3. Robust Fuzzy Noise Detection: The integration of a robust and powerful fuzzy noise detection scheme further contributes to the exceptional performance of the suggested method.

Table 2: Numerical results of the suggested method with related works using "Peppers" image.

Method	Noise density					
	10%		30%		50%	
	PSNR	MSE ($\times 10^{-2}$)	PSNR	MSE ($\times 10^{-2}$)	PSNR	MSE ($\times 10^{-2}$)
Noisy	18.30	1.4932	13.43	4.5994	11.15	7.7794
FMVMF	30.85	0.0822	21.53	0.7111	16.00	2.5806
HFC	29.89	0.1036	17.75	1.6909	12.94	5.1493
CAFSM	28.32	0.1528	26.04	0.2556	22.67	0.5519
DWM	31.40	0.0726	26.65	0.2164	22.44	0.5753
Proposed (gray)	34.81	0.0332	29.48	0.1146	25.62	0.2778
Proposed (color)	37.24	0.0191	30.82	0.0840	26.24	0.2397

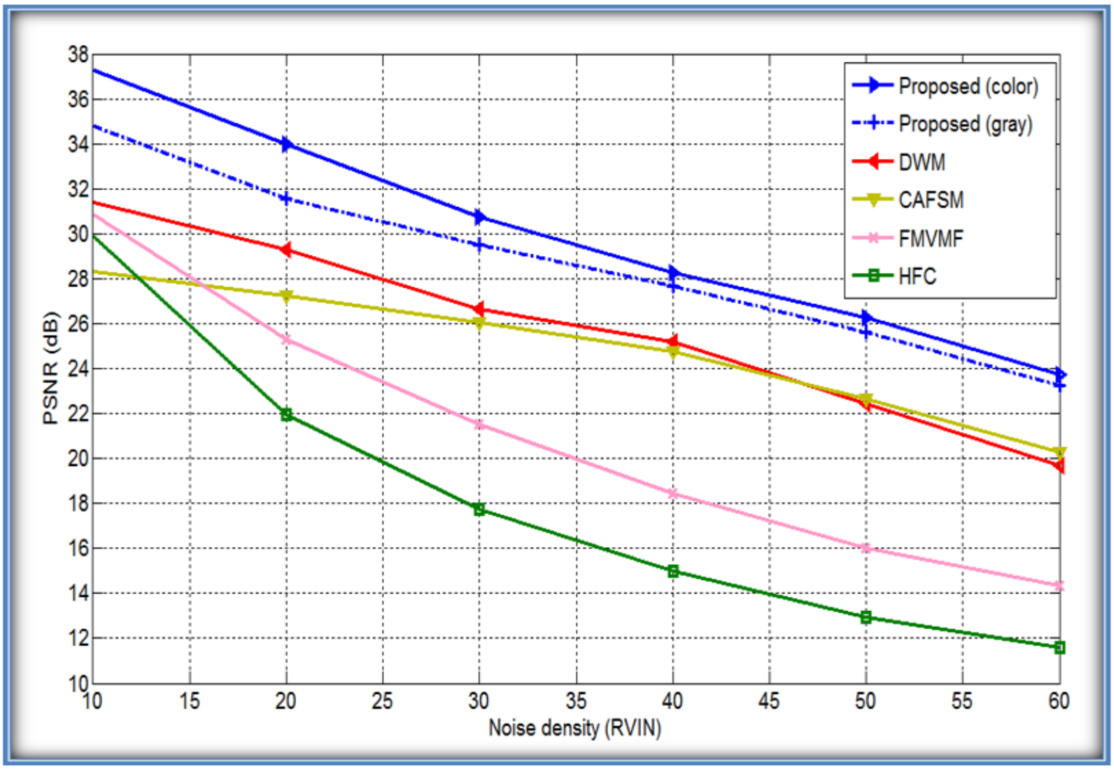

Fig. 3: Comparison chart in term of PSNR of the proposed color image algorithm with related works using the "Peppers" image corrupted with RVIN (10% - 60%).

IJDIAS International Journal of Discoveries and Innovations in Applied Sciences
| e-ISSN: 2792-3983 | www.openaccessjournals.eu | Volume: 3 Issue: 8

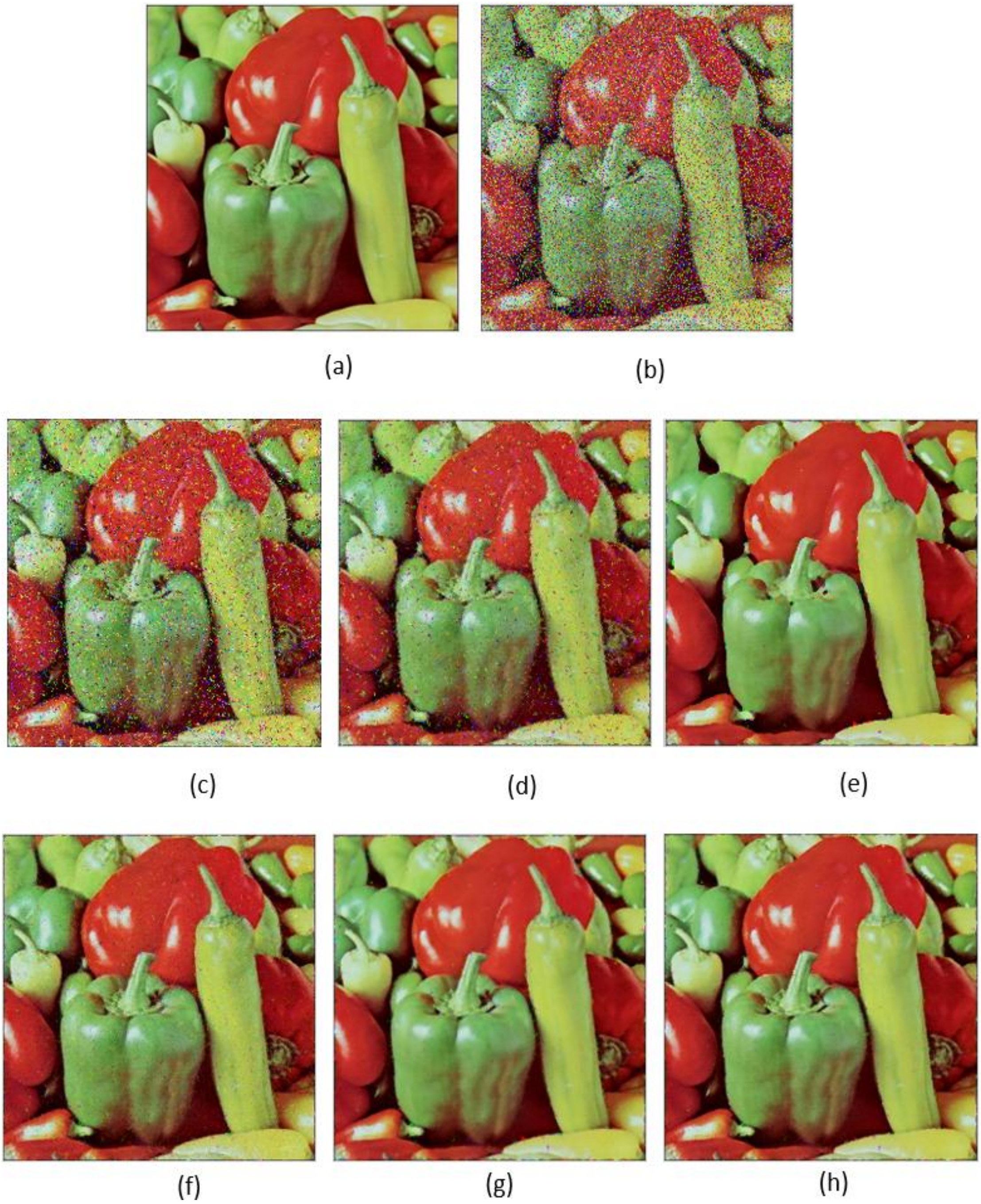

Fig. 4: Results of RVIN removing of "Peppers" image, (a) original image, (b) Noisy image corrupted with 30 % RVIN (PSNR: 13.43), (c) Processed image with HFC (PSNR: 17.75), (d) Processed image with FMVMF (PSNR: 21.53), (e) Processed image with CAFSM (PSNR: 26.04), (f) Processed image with DWM (PSNR: 26.65) (g) Processed image with the proposed gray image algorithm (PSNR: 29.48), (h) Processed image using the proposed color image algorithm (PSNR: 30.82).

5. Conclusion

This study suggests a new method for RVIN detection and reduction method for color image. The proposed method utilizes fuzzy logic, noise density estimation, and correlation between RGB

| e-ISSN: 2792-3983 | www.openaccessjournals.eu | Volume: 3 Issue: 8

components. The method capitalizes on the calculated noise density to dynamically determine an optimal window size for noise detection and shape the membership function employed in the noise detection process. Through comprehensive experimentation, the proposed method showcases exceptional performance surpassing numerous established impulse noise filtering techniques in both objective and subjective evaluations. Notably, the method excels in effectively removing noise while simultaneously preserving intricate image textures and details.

References

1. J. Chen, G. Zhang, S. Xu and H. Yu, "A Blind CNN Denoising Model for Random-Valued Impulse Noise," in IEEE Access, vol. 7, pp. 124647-124661, 2019.
2. C. Lin, Y. Li, S. Feng and M. Huang, "A Two-Stage Algorithm for the Detection and Removal of Random-Valued Impulse Noise Based on Local Similarity," in IEEE Access, vol. 8, pp. 222001-222012, 2020.
3. S. K. Maji and A. Mahajan, "A Joint Denoising Technique for Mixed Gaussian–Impulse Noise Removal in HSI," in IEEE Geoscience and Remote Sensing Letters, vol. 20, pp. 1-5, 2023.
4. P. H. Sangave and G. P. Jain, "Impulse noise detection and removal by modified boundary discriminative noise detection technique," 2017 International Conference on Intelligent Sustainable Systems (ICISS), Palladam, India, 2017, pp. 715-719.
5. T. M. Y. Shiju and A. V. N. Krishna, "A Two-Pass Hybrid Mean and Median Framework for Eliminating Impulse Noise From a Grayscale Image," 2021 2nd International Conference on Advances in Computing, Communication, Embedded and Secure Systems (ACCESS), Ernakulam, India, 2021, pp. 206-210.
6. W. K. Pratt, “Median filtering,” Image Proc. Institute, University of Southern California, Los Angeles, Tech. Rep., September 1975.
7. S. Deivalakshmi, S. Sarath and P. Palanisamy, "Detection and removal of Salt and Pepper noise in images by improved median filter," 2011 IEEE Recent Advances in Intelligent Computational Systems, Trivandrum, India, 2011, pp. 363-368, doi: 10.1109/RAICS.2011.6069335.
8. S.J. Ko, Y.H. Lee, “Center weighted median filters and their applications to image enhancement”, IEEE Trans. Circuits and Systems, Vol. (38), pp. (984–993), 1991
9. A. Sindhu and V. Radha, "A Novel Histogram Equalization Based Adaptive Center Weighted Median Filter for De-noising Positron Emission Tomography (PET) Scan Images," 2018 3rd International Conference on Communication and Electronics Systems (ICCES), Coimbatore, India, 2018, pp. 909-914, doi: 10.1109/CESYS.2018.8724108.
10. T. Chen and Hong Ren Wu, "Adaptive impulse detection using center-weighted median filters," in IEEE Signal Processing Letters, vol. 8, no. 1, pp. 1-3, Jan. 2001, doi: 10.1109/97.889633.
11. T. Rabie, "Hybrid mean adaptive center weighted median filter for color sensor denoising," Proceedings of 2004 International Symposium on Intelligent Signal Processing and Communication Systems, 2004. ISPACS 2004., Seoul, Korea (South), 2004, pp. 321-326, doi: 10.1109/ISPACS.2004.1439068.
12. F. J. Gallegos-Funes, B. E. Carvajal-Gamez, J. L. Lopez-Bonilla and V. I. Ponomaryov, "Steganographic method based on wavelets and center weighted median filter," 2010 INTERNATIONAL KHARKOV SYMPOSIUM ON PHYSICS AND ENGINEERING OF

MICROWAVES, MILLIMETER AND SUBMILLIMETER WAVES, Kharkiv, Ukraine, 2010, pp. 1-3, doi: 10.1109/MSMW.2010.5546011.

13. S. Salekin, S. Agaian, I. Jahan and S. Z. Sajal, "Image De-Noising Through Symmetric, Bell-Shaped, and Centered Weighted Median Filters Based Subband Decomposition," 2018 IEEE International Conference on Electro/Information Technology (EIT), Rochester, MI, USA, 2018, pp. 0493-0497, doi: 10.1109/EIT.2018.8500238.
14. V. Oliinyk, O. Ieremeiev and I. Djurović, "Center Weighted Median Filter Application to Time Delay Estimation in Non-Gaussian Noise Environment," 2019 IEEE 2nd Ukraine Conference on Electrical and Computer Engineering (UKRCON), Lviv, Ukraine, 2019, pp. 985-989, doi: 10.1109/UKRCON.2019.8879775.
15. A. Taguchi and N. Izawa, "Fuzzy center weighted median filters," 1996 8th European Signal Processing Conference (EUSIPCO 1996), Trieste, Italy, 1996, pp. 1-4.
16. M. M. Hamid, F. Fathi Hammad and N. Hmad, "Removing the Impulse Noise from Grayscaled and Colored Digital Images Using Fuzzy Image Filtering," 2021 IEEE 1st International Maghreb Meeting of the Conference on Sciences and Techniques of Automatic Control and Computer Engineering MI-STA, Tripoli, Libya, 2021, pp. 711-716.
17. V. Narayan, P. K. Mall, S. Awasthi, S. Srivastava and A. Gupta, "FuzzyNet: Medical Image Classification based on GLCM Texture Feature," 2023 International Conference on Artificial Intelligence and Smart Communication (AISC), Greater Noida, India, 2023, pp. 769-773.
18. P. V. S. Reddy, "Generalized Fuzzy Logic with twofold fuzzy set: Learning through Neural Net and Application to Business Intelligence," 2021 International Conference on Fuzzy Theory and Its Applications (iFUZZY), Taitung, Taiwan, 2021, pp. 1-5.
19. N. Kamide, "Sequential Fuzzy Description Logic: Reasoning for Fuzzy Knowledge Bases with Sequential Information," 2020 IEEE 50th International Symposium on Multiple-Valued Logic (ISMVL), Miyazaki, Japan, 2020, pp. 218-223.
20. H. M. Rehan Afzal, J. Yu and Y. Kang, "Impulse noise removal using fuzzy logics," 2017 32nd Youth Academic Annual Conference of Chinese Association of Automation (YAC), Hefei, China, 2017, pp. 413-418.
21. Dr. Muna M. Jawad, Dr. Ekbal H. Ali, Adel J. Yousif, “A Fuzzy Random Impulse Noise Detection and Reduction Method Based on Noise Density Estimation”, International Journal of Scientific & Engineering Research, Volume 5, Issue 3, March-2014.
22. C. Anjanappa and H. S. Sheshadri, "Development of mathematical morphology filter for medical image impulse noise removal," 2015 International Conference on Emerging Research in Electronics, Computer Science and Technology (ICERECT), Mandya, India, 2015, pp. 311-318, doi: 10.1109/ERECT.2015.7499033.
23. Y. Dong and S. Xu, “A New Directional Weighted Median Filter for Removal of Random-Valued Impulse Noise”, IEEE Signal Processing Letters, vol. (14), No. (3), pp. (193-196), March, 2007.
24. S. Schulte, V. De Witte, M. Nachtegael, D. Van Der Weken, E. E. Kerre, “Histogram-Based Fuzzy Colour Filter for Image Restoration”, Image and Vision Computing, Vol. (25), pp. (1377-1390), 2007.

25. J.Harikiran, B.Saichandana, B.Divakar "Impulse Noise Removal in Digital Images" International Journal of Computer Applications, Vol. (11), No. (8), pp. (39-42), November, 2010.
26. B. Smolka, M. Szczepanski, K.N. Plataniotis, and A.N. Venetsanopoulos, "Fast Modified Vector Median Filter", Computer Analysis of Images and Patterns, LNCS 2124, pp. (570-580), 2001.
27. Adel Jalal Yousif, "Image Steganography Based on Wavelet Transform and Color Space Approach", Diyala Journal of Engineering Sciences Vol (13) No 3, 2020: 23-34.
28. Fadhil Kadhim Zaidan Ghazwan Jabbar Ahmed, Adel Jalal Yousif, "A Digital Image Watermarking Scheme based on Discrete Cosine Transform", Journal of Engineering and Applied Sciences, vol. 4, issue 16, pp. 5762-5768, 2019.
29. Adel Jalal Yousif, "Image Steganography Based on Wavelet Transform and Color Space Approach", Diyala Journal of Engineering Sciences Vol (13) No 3, 2020: 23-34.
30. J. Moreno, B. Jaime and C. Fernandez, "NRPSNR: No-Reference Peak Signal-to-Noise Ratio for JPEG2000," 2013 Data Compression Conference, Snowbird, UT, USA, 2013, pp. 511-511, doi: 10.1109/DCC.2013.117.